

## Formation of ZnTe Nanowires by Oriented Attachment

Ken-Tye Yong,<sup>†,‡</sup> Yudhisthira Sahoo,<sup>†,§</sup> Hao Zeng,<sup>||</sup>  
Mark T. Swihart,<sup>\*,†,‡</sup> John R. Minter,<sup>#</sup> and  
Paras N. Prasad<sup>\*,†,§,||</sup>

*Institute for Lasers, Photonics and Biophotonics, Department of Chemical and Biological Engineering, Department of Chemistry, and Department of Physics, University at Buffalo, The State University of New York, Buffalo, New York 14260-4200, and Foundation Science and Technology Center, Eastman Kodak Company, Research Laboratories, Rochester, New York 14650*

Received April 9, 2007

Revised Manuscript Received June 21, 2007

### Introduction

One-dimensional nanostructures, such as semiconductor nanowires and nanorods, are a subject of intensive research because of their intriguing properties and great potential in technological applications ranging from optoelectronics to biology.<sup>1</sup> Semiconducting nanowires (NWs) are of particular interest because they may serve as key components of nanoscale electronic and photonic devices. Over the past several years, semiconductor NWs have been prepared using various synthetic methods, including the vapor–liquid–solid and solution–liquid–solid approaches, solvothermal methods, template-assisted growth, kinetic control of crystal growth direction, self-assembly, and thermolysis of a single-source precursor in ligating solvents.<sup>2,3</sup> For example, CdS, ZnS, Si, and Ge NWs have been grown by the vapor–liquid–solid process.<sup>4–6</sup> InP, CdSe, and PbSe NWs have been made by a solution–liquid–solid process using metal nanoparticle seeding.<sup>7,8</sup> Recently, our group has synthesized CdSe quantum rods,<sup>9</sup> PbSe quantum rods,<sup>10</sup> CdS nanoplatelets,<sup>11</sup> and PbS NWs<sup>12</sup> by hot colloidal methods using metal

nanoparticle seeding under conditions in which the seed particle does not melt.

Nanocrystals of many II–VI, III–V, and IV–VI semiconductors, including ZnS, ZnSe, CdSe, CdTe, InP, InAs, PbSe, and PbTe, have been extensively investigated in the past decade. However, reports on ZnTe nanocrystals are comparatively scarce. ZnTe is an attractive semiconductor with a direct band gap of 2.26 eV<sup>13</sup> and a Bohr exciton radius of 6.2 nm.<sup>14</sup> It has been suggested as a useful material in optoelectronic and thermoelectric devices, such as the first unit in a tandem solar cell, as a buffer layer for an HgCdTe infrared detector, or as part of the graded p-Zn(Te)Se multi-quantum-well structure in a blue-green laser diode.<sup>15–17</sup> ZnTe NW arrays have been synthesized by a pulsed electrochemical deposition method.<sup>14</sup> However, to date, there have been very few reports of ZnTe NWs prepared in solution.<sup>18</sup> Recently, Buhro's group has reported the synthesis of ZnTe NWs using the solution–liquid–solid (SLS) method.<sup>19</sup> Bismuth (Bi) nanoparticles were used to seed one-dimensional growth of ZnTe. However, the synthesis of Bi nanoparticles is not straightforward, and their reactivity to oxygen can further complicate their use. Thus, we report here an alternative method that does not use metallic nanoparticles.

In a typical experiment, zinc oxide (2 mmol), phenyl ether (5 mL), myristic acid (1.4 g), and hexadecylamine (3 g, ~12 mmol) were mixed and heated to 250 °C for 15–25 min under argon. Two milliliters of (TOP)Te solution (0.75 M Te in trioctylphosphine) was then rapidly injected into the hot mixture. The resulting light yellow-orange solution was held at 250 °C for 6–8 min before being gradually cooled to room temperature. The ZnTe NWs were precipitated by addition of chloroform followed by centrifugation. Further details are given in the Supporting Information. When using an oxide precursor like ZnO, a key process is complete precursor dissolution by formation of a soluble complex, most commonly involving a carboxylic acid. We found that relatively short-chain-length carboxylic acids such as myristic acid (C<sub>14</sub>H<sub>6</sub>O<sub>2</sub>) were more effective than longer-chain carboxylic acids (e.g., oleic acid) for dissolving the ZnO in phenyl ether in the presence of hexadecylamine. Apparently, these smaller ligands can better coordinate to Zn ions.<sup>20</sup> Hexadecylamine served as a coordinating surfactant in the synthesis and was necessary to achieve complete dissolution of the ZnO precursor. Control experiments showed that the

\* Corresponding author. E-mail: swihart@eng.buffalo.edu.

<sup>†</sup> Institute for Lasers, Photonics and Biophotonics, University at Buffalo.

<sup>‡</sup> Department of Chemical and Biological Engineering, University at Buffalo.

<sup>§</sup> Department of Chemistry, University at Buffalo.

<sup>||</sup> Department of Physics, University at Buffalo.

<sup>#</sup> Eastman Kodak Company.

- (1) Prasad, P. N., *Nanophotonics*; Wiley-Interscience: New York, 2004.
- (2) Cushing, B. L.; Kolesnichenko, V. L.; O'Connor, C. J. *Chem. Rev.* **2003**, *104*, 3893.
- (3) Wu, Y.; Yang, P. *J. Am. Chem. Soc.* **2001**, *123*, 3165.
- (4) Hanrath, T.; Korgel, B. A. *J. Am. Chem. Soc.* **2002**, *124*, 1424.
- (5) Holmes, J. D.; Johnston, K. P.; Doty, R. C.; Korgel, B. A. *Science* **2000**, *287*, 1471.
- (6) Barrelet, C. J.; Wu, Y.; Bell, D. C.; Lieber, C. M. *J. Am. Chem. Soc.* **2003**, *125*, 11498.
- (7) Hull, K. L.; Grebinski, J. W.; Kosel, T. H.; Kuno, M. *Chem. Mater.* **2005**, *17*, 4416.
- (8) Grebinski, J. W.; Hull, K. L.; Zhang, J.; Kosel, T. H.; Kuno, M. *Chem. Mater.* **2004**, *16*, 5260.
- (9) Yong, K.-T.; Sahoo, Y.; Swihart, M. T.; Prasad, P. N. *Adv. Mater.* **2006**, *18*, 1978.
- (10) Yong, K.-T.; Sahoo, Y.; Choudhury, K. R.; Swihart, M. T.; Minter, J. R.; Prasad, P. N. *Nano Lett.* **2006**, *6*, 709.
- (11) Yong, K.-T.; Sahoo, Y.; Swihart, M. T.; Prasad, P. N. *J. Phys. Chem. C* **2007**, *111*, 2447.
- (12) Yong, K.-T.; Sahoo, Y.; Choudhury, K. R.; Swihart, M. T.; Minter, J. R.; Prasad, P. N. *Chem. Mater.* **2006**, *18*, 5965.

- (13) Mahalingam, T.; John, V. S.; Rajendran, S.; Sebastian, P. J. *Semicond. Sci. Technol.* **2002**, *17*, 465.
- (14) Li, L.; Yang, Y.; Huang, X.; Li, G.; Zhang, L. *J. Phys. Chem. B* **2005**, *109*, 12394.
- (15) Kisker, D. W. *J. Cryst. Growth* **1989**, *98*, 127.
- (16) Kuhn, W. S.; Qu'Hen, B.; Gorochoy, O.; Triboulet, R.; Gebhardt, W. *Prog. Cryst. Growth Charact. Mater.* **1995**, *31*, 45.
- (17) Wilkerson, K. J.; Kappers, M. J.; Hicks, R. F. *J. Phys. Chem. A* **1997**, *13*, 2451.
- (18) Jun, Y.-w.; Choi, C.-S.; Cheon, J. *Chem. Commun.* **2000**, *1*, 101.
- (19) Wang, F.; Dong, A.; Sun, J.; Tang, R.; Yu, H.; Buhro, W. E. *Inorg. Chem.* **2006**, *45*, 7511.
- (20) Chen, H.-S.; Lo, B.; Hwang, J.-Y.; Chang, G.-Y.; Chen, C.-M.; Tasi, S.-J.; Wang, S.-J. *J. Phys. Chem. B* **2004**, *108*, 17119.

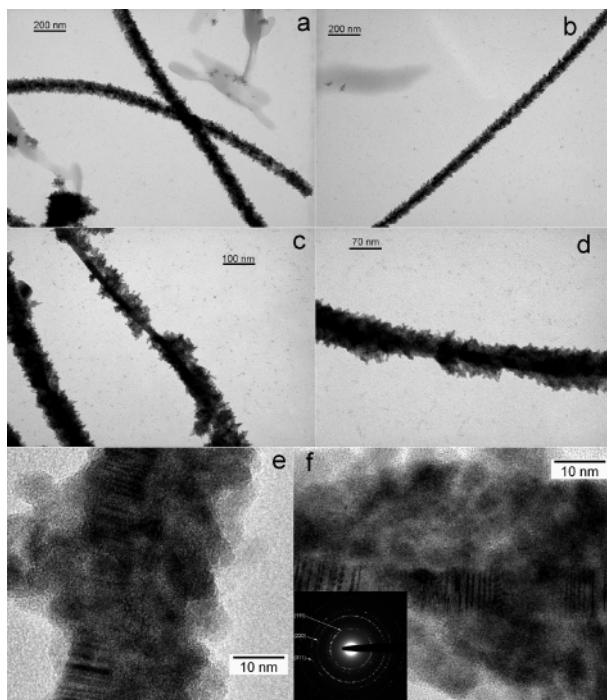


**Figure 1.** (a–d) TEM images and (e, f) HRTEM images of brushlike ZnTe nanowires.

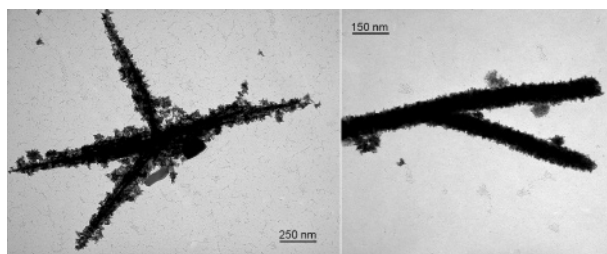
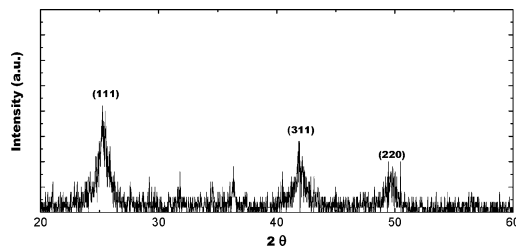


**Figure 2.** TEM images of branched ZnTe NWs.

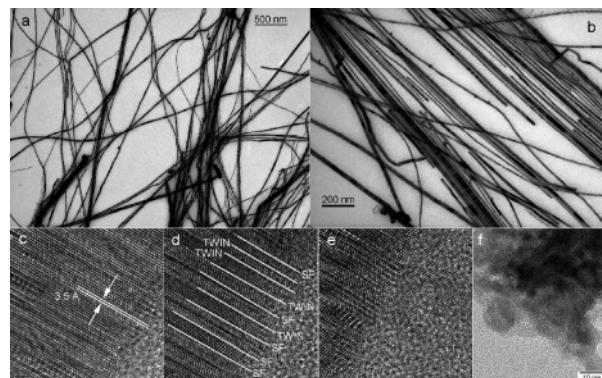
ZnO was not fully dissolved in solutions of myristic acid or other carboxylic acids that did not also contain an amine. In the presence of both surfactants, ZnO was completely dissolved above 220 °C and formed a homogeneous clear solution.

Figure 1 shows TEM images of ZnTe NWs prepared as described above. They have a brushlike appearance, with numerous bristles covering the surface of the wires. The wires are long and straight, with diameters from 70 to 100 nm and an average diameter of  $\sim 80$  nm. The NWs are typically  $>1 \mu\text{m}$  in length, and many are  $>5 \mu\text{m}$ . Bare patches where the bristles are absent and the inner core of the wire is visible were frequently observed, as shown in Figure 1c. The core diameter ranges from 10 to 25 nm, suggesting that the bristle layer has an average thickness of  $\sim 30$  nm. Free bristlelike ZnTe nanocrystals were also observed in the sample (see the Supporting Information). These may have detached from brushlike wires or they may have nucleated separately. In addition to straight NWs, branched and multibranching ZnTe NWs were observed (Figure 2), but constituted less than 4% of the overall product.

Images e and f in Figure 1 show HRTEM images of crystalline brushlike ZnTe NWs. The lattice fringe spacing is 3.5 Å, which corresponds to the (111) lattice planes of cubic ZnTe. In the core, these planes are aligned perpen-



**Figure 3.** XRD pattern from ZnTe nanowires like those shown in Figure 1.



**Figure 4.** (a, b) TEM images and (c, d) HRTEM images of smooth ZnTe nanowires, (e) HRTEM image of a ZnTe nanowire and an adjacent rod-shaped particle, and (f) HRTEM image of irregular ZnTe particles. In (d), “twin” indicates a twinning defect and “SF” indicates a stacking fault. A much larger version of (f) is available in the Supporting Information.

dicular to the NW axis, showing that it corresponds to the [111] direction. The inset shows a selected area electron diffraction (SAED) pattern from these NWs. The XRD pattern from the NWs (Figure 3) corresponds to the cubic zinc blende structure of ZnTe. Peak intensities are roughly consistent with random orientation, rather than the (111) orientation observed for the wire core. This is not surprising, considering that the bristles occupy a larger volume fraction than the core and that their crystallites are randomly oriented.

When dodecylamine (12 mmol), rather than hexadecylamine, was used as the cosurfactant along with myristic acid (1.4 g), smooth NWs were produced. TEM images of these NWs (Figure 4) show that they have an average diameter of 19 nm and typical lengths of more than  $1 \mu\text{m}$ . There was minimal diameter variation within a given wire, but significant wire-to-wire variations (diameter standard deviation of about 12 nm). ZnTe nanoparticles of irregular shape were also produced and made up 10–15% of the product. Some of these fused together, as shown in Figure 4f. HRTEM showed that the axis of the smooth NWs was aligned in the [111] direction of the cubic structure of ZnTe with an interplanar distance of 3.5 Å (Figure 4c). Careful examination of the ZnTe lattice planes reveals disruption of the lattice plane stacking in a large number of wires, indicating that the wires are not perfect single crystals. Planar defects such as dislocations, stacking faults, and twins have been identified, as shown in images d and e of Figure 4.

Jun et al.<sup>18</sup> reported that injecting a single-source precursor for ZnTe into a mixed-surfactant solution produced rodlike ZnTe nanocrystals. They proposed that the surfactants formed rodlike micelles that templated the one-dimensional crystal growth. Here, ZnTe NW formation is more likely to result

from an oriented attachment mechanism, in which rods or wires form by aggregation of small nanocrystals that each have a net dipole moment. This has been observed in other semiconductors, including CdSe,<sup>21</sup> ZnS,<sup>22</sup> CdTe,<sup>23</sup> and PbSe.<sup>24,25</sup> The process is driven by the reduction in surface area that occurs upon aggregation.<sup>22</sup> Recently, both theory and experiment have shown that the surface energy of the zinc-blende structure of ZnS is higher than that of the wurtzite structure in the nanoscale regime.<sup>26</sup> ZnTe, being isomorphous to ZnS, can exhibit similar polar termination of its {111} faces, leading to strong dipolar interactions between nanocrystals. These interactions can lead to oriented, rather than random, aggregation. In HRTEM images, several common features of oriented attachment were observed, including stacking faults and twinning defects that occur where individual nanocrystals merge.

The formation of the brushlike NWs rather than smooth NWs may stem from weaker binding of hexadecylamine to the nanocrystal surface compared to dodecylamine. Better-passivated nanocrystals will both grow and aggregate more slowly than nanocrystals with a more weakly bound surfactant. This allows more time for dipolar interactions to align the nanocrystals. When hexadecylamine is used, less completely passivated NCs may aggregate more rapidly, leading to decreased alignment and the formation of bristlelike structures by random aggregation. The appearance of the bristles on the brushlike structures is similar to the fractal structures that are produced by diffusion-limited aggregation that occurs among highly reactive particles. Thus, the brushlike nanowires seem to be composed of a core of well-aligned material upon which additional small particles have deposited with much reduced alignment.

An alternate possible mechanism for the formation of the wires is anisotropic growth, in which the presence of two surfactants with significantly different binding abilities to the NC faces may induce one-dimensional growth by leaving only one facet with appreciable growth rate. For example, strongly adsorbed phosphonic acid is known to slow the growth of CdSe nanocrystals and induce preferential growth along the *c*-axis of the wurtzite structure.<sup>27</sup> This produces rod-shaped CdSe nanocrystals. Rods with a high aspect ratio are obtained by maintaining a very high concentration of the precursors, often requiring the supply of precursors continuously or at multiple time points.<sup>28</sup> This growth mechanism has also been observed for CdTe and CdS.<sup>29</sup> Nonetheless, the aspect ratios in those systems have not been observed to approach wirelike dimensions. This is unlikely to be the mechanism of formation of the ZnTe nanowires described here, since only a fixed moderate concentration of precursors has been used in this study, and the aspect ratios of the wires produced here are much higher than those observed in the other nanorods that form by this mechanism.

**Acknowledgment.** This work was supported in part by the Chemistry and Life Sciences Directorate of the Air Force Office of Scientific Research (Grant #FA95550-06-1-0398) and National Science Foundation DMR-0547036. We also thank the National Center for Electron Microscopy at Lawrence Berkeley National Laboratory for providing access to the HRTEM facility.

**Supporting Information Available:** Detailed materials and methods; additional TEM and HRTEM of ZnTe nanowires and irregular nanoparticles. This material is available free of charge via the Internet at <http://pubs.acs.org>.

CM0709774

- 
- (21) Pradhan, N.; Xu, H.; Peng, X. *Nano Lett.* **2006**, *6*, 720.  
(22) Yu, J. H.; Joo, J.; Park, H. M.; Baik, S.-I.; Kim, Y. W.; Kim, S. C.; Hyeon, T. *J. Am. Chem. Soc.* **2005**, *127*, 5662.  
(23) Tang, Z.; Kotov, N. A.; Giersig, M. *Science* **2002**, *297*, 237.  
(24) Cho, K.-S.; Talapin, D. V.; Gaschler, W.; Murray, C. B. *J. Am. Chem. Soc.* **2005**, *127*, 7140.  
(25) Lu, W.; Gao, P.; Jian, W. B.; Wang, Z. L.; Fang, J. *J. Am. Chem. Soc.* **2004**, *126*, 14816.

- 
- (26) Zhang, H.; Huang, F.; Gilbert, B.; Banfield, J. F. *J. Phys. Chem. B* **2003**, *107*, 13051.  
(27) Peng, X.; Manna, L.; Yang, W.; Wickham, J.; Scher, E.; Kadavanich, A.; Alivisatos, A. P. *Nature* **2000**, *404*, 59.  
(28) Manna, L.; Scher, E. C.; Alivisatos, A. P. *J. Am. Chem. Soc.* **2000**, *122*, 12700.  
(29) Shieh, F.; Saunders, A. E.; Korgel, B. A. *J. Phys. Chem. B* **2005**, *109*, 8538.